Effect of Anisotropic Hybridization in YbAlB_{4} Probed by Linear Dichroism in Core-Level Hard X-Ray Photoemission Spectroscopy

Kentaro Kuga, Yuina Kanai, Hidenori Fujiwara, Kohei Yamagami, Satoru Hamamoto, Yuichi Aoyama, Akira Sekiyama, Atsushi Higashiya, Toshiharu Kadono, Shin Imada, Atsushi Yamasaki, Arata Tanaka, Kenji Tamasaku, Makina Yabashi, Tetsuya Ishikawa, Satoru Nakatsuji, and Takayuki Kiss

Phys. Rev. Lett. **123**, 036404 — Published 17 July 2019

DOI: 10.1103/PhysRevLett.123.036404

Effect of Anisotropic Hybridization in $YbAlB_4$ Probed by Linear Dichroism in Core-Level Hard X-ray Photoemission Spectroscopy

Kentaro Kuga,[1] Yuina Kanai,[1,2] Hidenori Fujiwara,[1,2] Kohei Yamagami,[1,2] Satoru Hamamoto,[1,2] Yuichi Aoyama,[1,2] Akira Sekiyama,[1,2] Atsushi Higashiya,[1,3] Toshiharu Kadono,[1,4] Shin Imada,[1,4] Atsushi Yamasaki,[1,5] Arata Tanaka,[6] Kenji Tamasaku,[1] Makina Yabashi,[1] Tetsuya Ishikawa,[1] Satoru Nakatsuji,[7,8] and Takayuki Kiss[1,2]

[1] *RIKEN SPring-8 Center, Sayo, Hyogo 679-5148, Japan.*
[2] *Graduate School of Engineering Science, Osaka University, Toyonaka, Osaka 560-8531, Japan.*
[3] *Faculty of Science and Engineering, Setsunan University, Neyagawa, Osaka 572-8508, Japan.*
[4] *College of Science and Engineering, Ritsumeikan University, Kusatsu, Shiga 525-8577, Japan.*
[5] *Faculty of Science and Engineering, Konan University, Kobe, Hyogo 658-8501, Japan.*
[6] *Department of Quantum Matter, ADSM, Hiroshima University, Higashi-Hiroshima, Hiroshima 739-8530, Japan.*
[7] *The Institute for Solid State Physics, The University of Tokyo, Kashiwa, Chiba 277-8581, Japan.*
[8] *CREST, Japan Science and Technology Agency (JST), 4-1-8 Honcho Kawaguchi, Saitama 332-0012, Japan.*

(Dated: May 22, 2019)

We have probed the crystalline electric-field ground states of pure $|J = 7/2, J_z = \pm 5/2\rangle$ as well as the anisotropic c-f hybridization in both valence fluctuating systems α- and β-$YbAlB_4$ by linear polarization dependence of angle-resolved core level photoemission spectroscopy. Interestingly, the small but distinct difference between α- and β-$YbAlB_4$ was found in the polar angle dependence of linear dichroism, indicating the difference in the anisotropy of c-f hybridization which may be a key to understand a heavy Fermi liquid state in α-$YbAlB_4$ and a quantum critical state in β-$YbAlB_4$.

Crystalline electric field (CEF) ground state (GS) regulates physical properties at low temperatures and sometimes leads to variety of nontrivial quantum states such as quantum criticality in quadrupolar Kondo lattice system [1–3], colossal magnetoresistance and high temperature superconductivity in transition metal oxide [4]. For example in high T_c cuprate, CEF splitting of Cu $3d$ electron determines the half filling in $d_{x^2-y^2}$ orbital, which anisotropically hybridizes with neighboring O $2p$ electrons, mediating electric and magnetic interaction [5]. Such an anisotropic hybridization of the orbital selected by CEF plays essential role of the physical properties in many of transition metal oxides [4]. Accurate estimation of CEF GS and hybridization is indispensable to understand the underlying mechanisms.

In rare earth metal systems, it is essential to determine the CEF GS yielding rich variety of the unconventional low temperature properties. One of the most interesting phenomena is a quantum criticality in β-$YbAlB_4$ which stems from the "pure" $|J = 7/2, J_z = \pm 5/2\rangle$ CEF GS and the nodal hybridization in momentum space as predicted by A. Ramires, *et al.* [6]. In this theory, a new type of topological phase transition in Fermi surface is predicted to arise and induces a topological non-trivial vortex metal which shows magnetic properties of $T^{-1/2}$ divergence and T/B scaling.

β-$YbAlB_4$ is a fascinating and mysterious material which is the firstly discovered superconductor in Yb-based heavy fermion systems [7, 8] and shows quantum criticality without tuning [9] in the strongly valence fluctuating state [10]. Furthermore, the quantum criticality at ambient pressure survives up to 0.4 GPa, forming a non-Fermi-liquid phase [11]. As a function of pressure, β-$YbAlB_4$ forms non-Fermi-liquid phase including the quantum criticality at ambient pressure [11]. To understand the underlying mechanism, laser ARPES probed anisotropic hybridization as a momentum dependent Kondo hybridization band which is consistent with nodal hybridization model [12]. CEF GS is also reported to be consistent with $|\pm 5/2\rangle$ state estimated by the temperature dependence of magnetic susceptibility [13]. Indeed, $|\pm 5/2\rangle$ state is plausible because the distribution of $4f$ hole extends toward neighboring heptagonal rings of boron atoms, maximizing the hybridization with boron rings. However, the analysis of the temperature dependence of magnetic susceptibility is not straightforward because β-$YbAlB_4$ have strong valence fluctuation due to the strong c-f hybridization [10]. Low symmetric orthorhombic crystal structure in β-$YbAlB_4$ also makes it quite difficult to analyze CEF accurately because of many of the CEF parameters. Thus, no definitive experimental results including the estimation of the admixture with other J_z components are reported.

Recently the CEF GSs of several Lanthanide based materials have been probed by the angle-resolved core-level hard x-ray photoemission spectroscopy (HAXPES) using linearly polarized light. Linear dichroism (LD), which is defined as the spectral difference of the photoemission spectra obtained by the s- and p-polarized configuration as shown in Fig. 1(b), reflects the anisotropic charge distribution of the $4f$ hole through the interaction with the core hole created in the optical process [16]. For example in Yb based materials, LDs of Yb $3d$ core-level multiplet structures determined the GSs of cubic system YbB_{12} as Γ_8 and the GSs of tetragonal systems $YbRh_2Si_2$ and $YbCu_2Si_2$ as $|\pm 3/2\rangle$ and $-0.36|\pm 5/2\rangle + 0.93|\mp 3/2\rangle$,

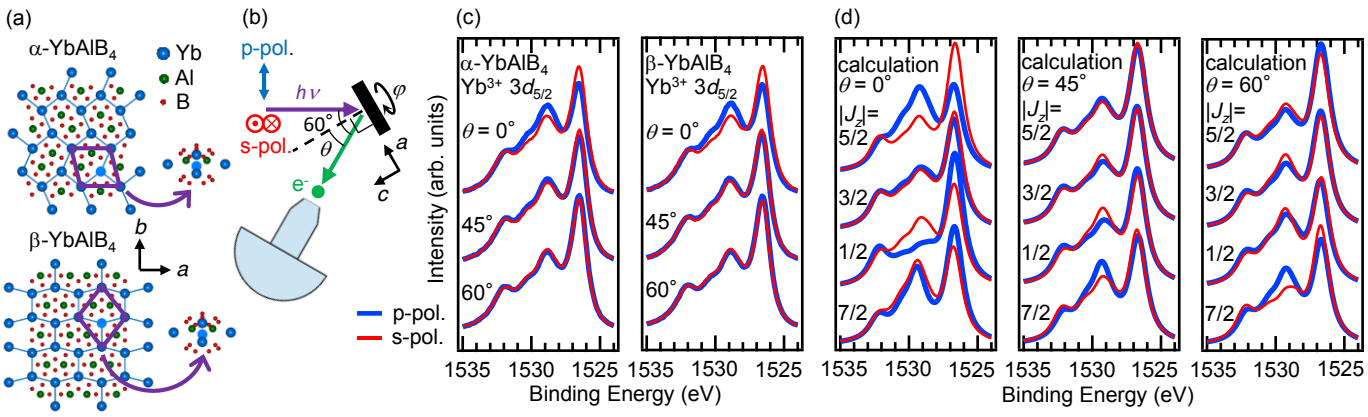

FIG. 1. (a) Crystal structure of α- and β-$YbAlB_4$ with a view along c-axis. Yb-Al layer is sandwiched by heptagonal and pentagonal B layers, respectively. The local structures surrounded by the purple quadrangles are shown at the right side as the pictorial views which are oriented to the acute angles of the quadrangles. (b) Schematic top view geometry of incident horizontally (blue arrow) and vertically (red arrow) polarized X-rays, sample and photoelectron analyzer. Polar angle θ is defined as an angle between the directions toward the photoelectron analyzer and c-axis of the sample, and $\theta = 60^\circ$ corresponds that the c-axis is oriented toward incident X-ray. Azimuthal angle φ is defined as the angle of the rotation along c-axis and $\varphi = 0^\circ$ corresponds to the geometry as drawn in Fig. 1(b). (c) Polarization-dependent Yb^{3+} $3d_{5/2}$ core-level HAXPES spectra of α- and β-$YbAlB_4$ with the polar angle of $\theta = 0^\circ$, 45° and 60°. Red thin and blue thick lines correspond to s- and p-polarization. The spectra are normalized by the spectral weight of Yb^{3+} $3d_{5/2}$ after the subtraction of Shirley-type backgrounds [14, 15]. (d) Ionic calculation of polarization-dependent Yb $3d_{5/2}$ core-level HAXPES spectra of pure J_z states of $4f$ hole at each θ.

respectively [17, 18]. This method is also applicable to the lower symmetric systems. In this letter, we show the experimental evidence of pure $|\pm 5/2\rangle$ CEF GS of the orthorhombic β-$YbAlB_4$ probed by polar angle and azimuthal angle dependence of LDs of Yb $3d$ HAXPES spectra. In addition, we found the importance of explicit anisotropic hybridization between $4f$ and conduction electrons to describe the CEF of β-$YbAlB_4$. For comparison, we also measured stoichiometric compound α-$YbAlB_4$ which shows heavy Fermi liquid ground state [19].

In α- and β-$YbAlB_4$, local symmetry at Yb site is C_s and C_{2v}, respectively [20]. However, the regions surrounded by the four neighboring Yb sites resemble in both systems as shown in the purple quadrangles and their pictorial views in Fig. 1(a). Therefore, we can approximate that the local symmetry at Yb site in α-$YbAlB_4$ is C_{2v} and similar CEF GS is expected, which is turned out to be true later. $J = 7/2$ states of Yb^{3+} $4f$ electron in C_{2v} symmetry will split into four doublets and C_{2v} CEF is expressed by B_2^0, B_2^2, B_4^0, B_4^2, B_4^4, B_6^0, B_6^2, B_6^4 and B_6^6 in Stevens formalism [21]. These parameters will produce the eight eigenfunctions expressed by using J_z as $a_i|\pm 5/2\rangle + b_i|\mp 3/2\rangle + c_i|\pm 1/2\rangle + d_i|\mp 7/2\rangle (i = 1 \sim 4)$, where $a_i^2 + b_i^2 + c_i^2 + d_i^2 = 1$. For the simple comparison between measurement and calculation, we have performed ionic calculation including the full multiplet theory and the local CEF splitting using the XTLS 9.0 program [22, 23]. Atomic parameters such as the $4f$-$4f$ and $3d$-$4f$ Coulomb and exchange interactions (Slater integrals) and the spin-orbit couplings was obtained using Cowan's code based on the Hartree-Fock method [24]. The Slater integrals and spin-orbit couplings are reduced to 88% and 98% according to the references [17, 18, 25]. Single impurity Anderson model (SIAM) was also employed for the calculation which include explicit c-f hybridization [26, 27].

We performed polarization-dependent Yb $3d$ core-level HAXPES with a MBS A1-HE hemispherical photoelectron spectrometer at BL19LXU of SPring-8 [28, 29]. Horizontally polarized X-ray radiation produced by 27 m long undulator was monochromated to be 7.9 keV by a Si(111) double-crystal and a Si(620) channel-cut crystal. To switch the excitation light from horizontal to vertical polarization for LD, we used two diamond(100) single crystals as a phase retarder and vertically polarized component of the X-ray was 98% [30]. Since the direction of the photoelectron analyzer was in the horizontal plane with an angle about incident X-ray of 60° as shown in Fig. 1(b), horizontally polarized and vertically polarized X-rays correspond to s- and p-polarization geometry, respectively. The details of sample preparation and characterization are described in Supplemental Materials [31]. The experimental geometry was controlled by using a two-axis manipulator which equips polar and azimuthal rotations [30]. The energy resolution was set to $\sim$ 400 meV. The sample temperature was set to 25 K, which is sufficiently lower than the first excited energy confirmed by negligible temperature dependence up to 60 K for β-$YbAlB_4$ (see Supplemental Materials for

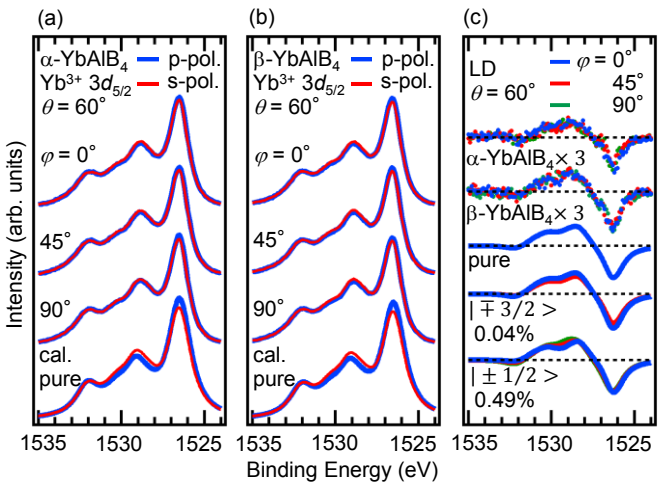

FIG. 2. (a) and (b) The azimuthal angle dependence of Yb^{3+} $3d_{5/2}$ core-level HAXPES spectra in α- and β-$YbAlB_4$ at $\theta = 60^\circ$ and the ionic calculation of pure $|\pm 5/2\rangle$ state. (c) The azimuthal angle dependence of LDs in α- and β-$YbAlB_4$ (closed circle) and the ionic calculation for pure $|\pm 5/2\rangle$ state and $|\pm 5/2\rangle$ plus a small amount of $|\mp 3/2\rangle$ ($\sim 0.9998|\pm 5/2\rangle + 0.02|\mp 3/2\rangle$) or $|\pm 1/2\rangle$ ($\sim 0.9975|\pm 5/2\rangle + 0.07|\pm 1/2\rangle$) state (solid line). LD is defined as the difference of normalized intensity between s- and p-polarization. The amplitude of LDs of α- and β-$YbAlB_4$ is multiplied by three to compare with the calculations.

detail [32]).

Figure 1(c) is the polarization-dependent Yb^{3+} $3d_{5/2}$ core-level HAXPES spectra of α- and β-$YbAlB_4$ with polar angle of $\theta = 0^\circ$, 45° and 60° as drawn in Fig. 1(b). The multiplet structures peak at 1526, 1529 and 1532 eV with polarization and θ dependences which reflect the charge distribution of $4f$ holes. The polarization and θ dependences in α- and β-$YbAlB_4$ are similar, suggesting almost the same CEF GS as expected from the local arrangement of neighboring atoms (Fig. 1(a)). Peaks at 1526 eV with s-polarization geometry (s-pol.) are higher than those of the p-polarization geometry (p-pol.) at $\theta = 0^\circ$. This difference becomes smaller at 45° and the sign changes at 60°. For the peaks at 1529 eV, these magnitude relations are reversed. According to the ionic calculation shown in Fig.1 (d), all the magnitude relations in addition to the comparably large LD at $\theta = 0^\circ$ are consistent with only $|\pm 5/2\rangle$ state. However, the magnitude of the LDs are about 3 times smaller than those of ionic calculation at $\theta = 0^\circ$ and 60°. These comparisons suggest that the main component of the wave functions in α- and β-$YbAlB_4$ is $|\pm 5/2\rangle$. The possible reasons for the quantitative differences are the admixture with other J_z components and/or c-f hybridization because both effects will deform the charge distribution of $4f$ hole and will change LD. The other extrinsic reasons such as back-scattering effect of the photoelectrons [33] are discussed in Supplemental Materials and all of their effects are turned out to be negligibly small [34].

Firstly, we focus on the mixing effect, namely $|\pm 5/2\rangle$ plus $|\mp 3/2\rangle$, $|\pm 1/2\rangle$ and/or $|\mp 7/2\rangle$. Pure $|\pm 5/2\rangle$ state shows no rotational dependence in LDs along c-axis as shown in Fig. 2(c) because of the isotropic charge distribution around c-axis. On the other hand, mixed states induce the azimuthal angle dependence as shown in $CeCu_2Ge_2$ [35] except the binary mixed state with $|\mp 7/2\rangle$. However, it is unnatural if the wave function is $|\pm 5/2\rangle$ plus $|\mp 7/2\rangle$ because CEF Hamiltonian must have tetragonal symmetric terms of pure $|\pm 5/2\rangle$ state plus the six-fold symmetric term B_6^6 and other orthorhombic terms B_2^2, B_4^2 and B_6^2 must be zero. Therefore we can distinguish if the CEF GS is pure $|\pm 5/2\rangle$ state or mixed state by measuring the azimuthal angle dependence of LDs.

Figure 2(a), (b) and (c) show the Yb^{3+} $3d_{5/2}$ core-level HAXPES spectra with different azimuthal angles φ and with the fixed polar angle of $\theta = 60^\circ$ in α-$YbAlB_4$, β-$YbAlB_4$ and their LDs, respectively. For both α- and β-$YbAlB_4$, the azimuthal angle dependences of LD are negligible within the experimental noise, indicating the pure $|\pm 5/2\rangle$ state. The error bars of the wave function can be estimated by ionic calculation for the binary mixed states as shown in Fig. 2(c). In case of $|\pm 5/2\rangle$ plus (minus) $|\mp 3/2\rangle$ state, four fold symmetric azimuthal angle dependence appears and LDs at $\varphi = 0^\circ$ and 90° overlap and LD at $\varphi = 45^\circ$ is smaller (larger) than others. The azimuthal angle dependence is very sensitive and experimental statistics suggests that the maximum possible component of $|\mp 3/2\rangle$ is only 0.04%, indicating that LD by HAXPES is an extremely sensitive probe of electronic state. On the other hand, $|\pm 5/2\rangle$ plus (minus) $|\pm 1/2\rangle$ state must show two fold symmetry in the azimuthal angle dependence of LDs, and LD at 1529 eV increases (decreases) as φ changes from 0° to 90°. Since the azimuthal angle dependence is less sensitive within the experimental statistics, the maximum possible component of $|\pm 1/2\rangle$ is estimated as 0.49%. If $|\mp 3/2\rangle$ and/or $|\pm 1/2\rangle$ are mixed in addition to $|\mp 7/2\rangle$, $|\mp 7/2\rangle$ can have a finite contribution because orthorhombic CEF parameters of B_2^2, B_4^2 and B_6^2 do not have to be all zero which is contrasting to the binary mixed state with $|\mp 7/2\rangle$ as we explained above. However, the contribution would be much smaller than that of $|\mp 3/2\rangle$ and/or $|\pm 1/2\rangle$ states, resulting in the error bar much less than that of $|\mp 3/2\rangle$ or $|\mp 1/2\rangle$. As these tiny error bars cannot explain the huge difference of LDs between the experiment and calculation by ionic model, we can conclude that the LDs in α- and β-$YbAlB_4$ are modified by c-f hybridization. Note that the c-f hybridization must be φ independent because the anisotropy in c-f hybridization will yield anisotropic LDs.

As α- and β-$YbAlB_4$ are strongly valence fluctuating systems with the Yb valences of 2.73 and 2.75 [10], strong c-f hybridization is expected to modify LD, which

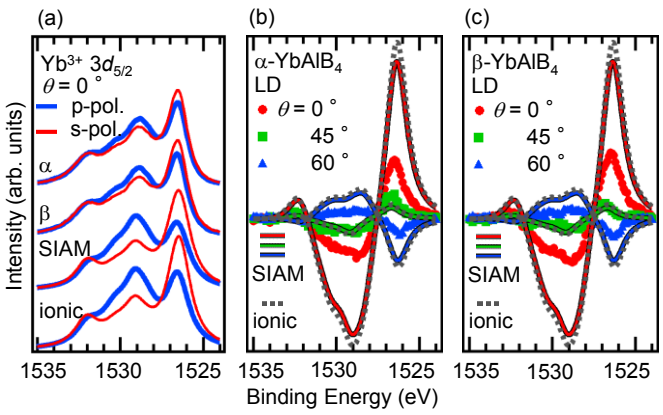

FIG. 3. (a) Polarization-dependent Yb^{3+} $3d_{5/2}$ core-level HAXPES spectra of α- and β-$YbAlB_4$ at $\theta = \varphi = 0°$, and the calculation of the spectra for $|\pm 5/2\rangle$ state based on SIAM including isotropic c-f hybridization. (b) and (c) The experimental LDs (closed circle, square and triangle) of α- and β-$YbAlB_4$ and the calculation for $|\pm 5/2\rangle$ state based on SIAM (solid line) and ionic model (broken line). Red, green and blue lines on the black lines correspond to the LDs by SIAM at $\theta = 0°$, $45°$ and $60°$. Same parameters are used in the calculation shown in (b) and (c).

was not apparently observed in YbB_{12}, $YbRh_2Si_2$ and $YbCu_2Si_2$ [17, 18]. To take into account the mixed valence state between Yb^{3+} ($4f^{13}$) and Yb^{2+} ($4f^{14}\underline{L}$), where $\underline{L}$ denotes the conduction band with one hole, the calculation based on SIAM for $|\pm 5/2\rangle$ state has been employed with isotropic c-f hybridization. Figure 3(a) shows the Yb^{3+} $3d_{5/2}$ core-level HAXPES spectra of α-$YbAlB_4$, β-$YbAlB_4$ and calculation by SIAM and ionic model at $\theta = \varphi = 0°$. The parameters of the Coulomb interaction between the $4f$ electrons and $3d$ core hole U_{fc} and the effective $4f$ binding energy Δ_f and isotropic c-f hybridization strength $V_{\rm eff}$ were set to be 10.0, 0.5 and 1.0 eV. The peaks of multiplet by SIAM is slightly wider than those of ionic model and the multiplet structure will drastically change if the $V_{\rm eff}$ is larger than 2.0 eV (not shown). Figure 3(b) and (c) show experimental LDs of α- and β-$YbAlB_4$ and the calculated LDs by SIAM and ionic model. For all geometry, calculations by SIAM show 1.15 times smaller LDs than that of ionic model. The ratio of the integrated intensity of LDs from 1528 to 1534 eV between experiments of α-$YbAlB_4$ (β-$YbAlB_4$) and calculations by SIAM with isotropic hybridization are 2.9 (2.6), 0.68 (1.0), and 3.6 (3.2) for $\theta = 0°$, $45°$ and $60°$, respectively. These comparisons indicate the importance of anisotropic c-f hybridization to understand the CEF in α- and β-$YbAlB_4$ which easily deforms the charge distribution as well as the LDs like oxides. Furthermore we can see the larger anisotropy in LDs of α-$YbAlB_4$, indicating the different anisotropy in c-f hybridization which is integrated into CEF.

Our experiments of α- and β-$YbAlB_4$ have probed the CEF GSs of pure $|\pm 5/2\rangle$ with the polar angle θ dependent and azimuthal angle φ independent c-f hybridizations. These results remind us the topological nontrivial vortex metallic state originating from nodal hybridization in momentum space, which is predicted in β-$YbAlB_4$ [6]. Experimental support in this nodal hybridization has been reported that laser ARPES measurement for β-$YbAlB_4$ probed two anticrossings of $4f$ CEF levels with dispersive conduction band which momentum dependence is consistent with nodal hybridization model [12]. On the other hand, for α-$YbAlB_4$, no clear Kondo hybridization band like β-$YbAlB_4$ was observed by laser ARPES. In our measurement of LD for α-$YbAlB_4$, we observed clear c-f hybridization in Yb $4f$ $|\pm 5/2\rangle$ state possibly because Yb $3d_{5/2}$ core-level HAXPES reflects local feature compared with valence band measured by ARPES. Furthermore, we discovered that the LD at each θ in β-$YbAlB_4$ has a slightly smaller deviation from calculation than the LD in α-$YbAlB_4$ as shown in Fig. 3(b) and (c), indicating that β-$YbAlB_4$ has the slightly smaller anisotropy of c-f hybridization. Our establishment of the similarity in the CEF GSs of pure $|\pm 5/2\rangle$ with very small error bars of less than 0.5% and the subtle difference in anisotropic c-f hybridization will help finding the key point to understand the mechanism of the quantum critical state in β-$YbAlB_4$ and the Fermi liquid state in α-$YbAlB_4$. Furthermore, our solution of an accurate probe for CEF GS in strongly valence fluctuating and Yb-based low symmetric system is attractive to other strongly correlated electron systems such as α-$YbAl_{1-x}Fe_xB_4$ and Yb-Al-Au approximant crystal and quasicrystal [36, 37]. As we have shown the existence of anisotropy in c-f hybridization, the detailed angle resolved core level LDs by HAXPES can be a new probe of anisotropic c-f hybridization in real space.

We thank S. Fujioka, H. Aratani, T. Hattori, H. Yomosa, S. Takano, T. Kashiuchi, K. Nakagawa, K. Sakamoto and Y. Kobayashi for support in experiments. We also thank H. Kobayashi for useful discussions. Sample preparation was carried out under the Visiting Researcher's Program of the Institute for Solid State Physics, the University of Tokyo. HAXPES experiments were performed at BL19LXU in SPring-8 with the approval of RIKEN (proposal nos. 20160034, 20160066, 20170043, 20170081, 20180026 and 20180076). This work is supported by by a Grant-in-Aid for Scientific Research (16H04014, 16H04015, 18K03512), and a Grant-in-Aid for Innovative Areas (16H01074, 18H04317) from MEXT and JSPS, Japan. This work is partially supported by CREST (JPMJCR15Q5,JPMJCR18T3), Japan Science and Technology Agency, by Grants-in-Aid for Scientific Research (16H02209), and by Grants-in-Aids for Scientific Research on Innovative Areas (15H05882, 15H05883) from MEXT. Y.K. was supported by the JSPS Research Fellowships for Young Scientists.

[1] D. L. Cox, Phys. Rev. Lett. **59**, 1240 (1987).
[2] D. L. Cox and M. Makivic, Physica B **199**, 391 (1994).
[3] H. Kusunose, K. Miyake, Y. Shimizu, and O. Sakai, Phys. Rev. Lett. **76**, 271 (1996).
[4] Y. Tokura and N. Nagaosa, Science **288**, 462 (2000).
[5] F. C. Zhang and T. M. Rice, Phys. Rev. B **37**, 3759(R) (1988).
[6] A. Ramires, P. Coleman, A. H. Nevidomskyy, and A. M. Tsvelik, Phys. Rev. Lett. **109**, 176404 (2012).
[7] S. Nakatsuji *et al.*, Nature Phys. **4**, 603 (2008).
[8] K. Kuga, Y. Karaki, Y. Matsumoto, Y. Machida, and S. Nakatsuji, Phys. Rev. Lett. **101**, 137004 (2008).
[9] Y. Matsumoto, S. Nakatsuji, K. Kuga, Y. Karaki, N. Horie, Y. Shimura, T. Sakakibara, A. Nevidomskyy, and P. Coleman, Science **331**, 316 (2011).
[10] M. Okawa *et al.*, Phys. Rev. Lett. **104**, 247201 (2010).
[11] T. Tomita, K. Kuga, Y. Uwatoko, P. Coleman, and S. Nakatsuji, Science **349**, 506 (2015).
[12] C. Bareille, S. Suzuki, M. Nakayama, K. Kuroda, A. H. Nevidomskyy, Y. Matsumoto, S. Nakatsuji, T. Kondo, and S. Shin, Phys. Rev. B **97**, 045112 (2018).
[13] A. H. Nevidomskyy and P. Coleman, Phys. Rev. Lett. **102**, 077202 (2009).
[14] D. A. Shirley, Phys. Rev. B **5**, 4709 (1972).
[15] A. Proctor and P. M. A. Sherwood, Anal. Chem. **54**, 13 (1982).
[16] A. Sekiyama, Y. Kanai, A. Tanaka, and S. Imada, J. Phys. Soc. Jpn. **88**, 013706 (2019).
[17] T. Mori *et al.*, J. Phys. Soc. Jpn. **83**, 123702 (2014).
[18] Y. Kanai *et al.*, J. Phys. Soc. Jpn. **84**, 073705 (2015).
[19] Y. Matsumoto, K. Kuga, T. Tomita, Y. Karaki, and S. Nakatsuji, Phys. Rev. B **84**, 125126 (2011).
[20] R. T. Macaluso, S. Nakatsuji, K. Kuga, E. L. Thomas, Y. Machida, Y. Maeno, Z. Fisk, and J. Y. Chan, Chem. Mater. **19**, 1918 (2007).
[21] K. W. H. Stevens, Proc. Phys. Soc. Sec. A **65**, 209 (1952).
[22] B. T. Thole, G. van der Laan, J. C. Fuggle, G. A. Sawatzky, R. C. Karnatak, and J.-M. Esteva, Phys. Rev. B **32**, 5107 (1985).
[23] A. Tanaka and T. Jo, J. Phys. Soc. Jpn. **63**, 2788 (1994).
[24] R. D. Cowan, *The Theory of Atomic Structure and Spectra* (University of California Press, 1981).
[25] J. Yamaguchi *et al.*, Phys. Rev. B **79**, 125121 (2009).
[26] O. Gunnarsson and K. Schönhammer, Phys. Rev. B **28**, 4315 (1983).
[27] J.-M. Imer and E. Wuilloud, Zeitsch. Phys. B: Condens. Matter **66**, 153 (1987).
[28] M. Yabashi *et al.*, Nucl. Instrum. and Methods in Phys. Res. A **467-468**, 678 (2001).
[29] M. Yabashi, K. Tamasaku, and T. Ishikawa, Phys. Rev. Lett. **87**, 140801 (2001).
[30] H. Fujiwara *et al.*, J. Synchrotron Radiat. **23**, 735 (2016).
[31] See Supplemental Material at [*URL will be inserted by publisher*] for the sample preparation and the characterization, which also includes Ref. [20].
[32] See Supplemental Material at [*URL will be inserted by publisher*] for the evidence of the negligible temperature dependence of LD, which also includes Ref. [17, 19].
[33] J. Weinen *et al.*, J. Elec. Spec. and Rel. Phen. **198**, 6 (2015).
[34] See Supplemental Material at [*URL will be inserted by publisher*] for the candidates of the extrinsic reason for the suppression of LD, which also includes Ref. [16, 19, 23, 33, 38–40].
[35] H. Aratani, Y. Nakatani, H. Fujiwara, M. Kawada, Y. Kanai, K. Yamagami, S. Fujioka, S. Hamamoto, K. Kuga, *et al.*, Phys. Rev. B **98**, 121113(R) (2018).
[36] K. Kuga *et al.*, Science Advances **4**, eaao3547 (2018).
[37] K. Deguchi, S. Matsukawa, N. Sato, T. Hattori, K. Ishida, H. Takakura, and T. Ishimasa, Nature Materials **11**, 1013 (2012).
[38] S. M. Goldberg, C. S. Fadley, and S. Kono, J. Electron Spectrosc. Relat. Phenom. **21**, 285 (1980).
[39] M. B. Trzhaskovskaya, V. I. Nefedov, and V. G. Yarzhemsky, At. Data Nucl. Data Tables **77**, 97 (2001).
[40] M. B. Trzhaskovskaya, V. K. Nikulin, V. I. Nefedov, and V. G. Yarzhemsky, At. Data Nucl. Data Tables **92**, 245 (2006).